Tailoring tripodal ligands for zinc sensing

Zhaohua Dai*[a] and James W. Canary*[b]

Received (in Montpellier, France) 17th July 2007, Accepted 28th August 2007
First published as an Advance Article on the web 11th September 2007
DOI: 10.1039/b710803f

Zinc plays an important role in biological processes. It is implicated in many diseases, including those affecting the brain. Imaging zinc is becoming crucial to the elucidation of zinc concentration, distribution, kinetics and functions in cells and tissues. This review highlights recent advances in the development of picolylamine-based tripodal compounds as zinc sensors, especially our work in the field of sensing "invisible" Zn(II) using steady-state fluorescence, fluorescence lifetimes and chiroptical spectroscopy. Our approach has emphasized creative ligand design and detection schemes. Utilizing tris(2-pyridylmethyl)amine-based N_4 tripodal ligands has provided a flexible system for engineering zinc sensors with improved sensitivity, selectivity and contrast. Also included are results with tripodal ligands that have focused more on applications.

Introduction

Zinc in biology

The coordination sphere of Zn(II) can accommodate the demands of various ligands: It has a d^{10} electronic configuration and offers no crystal field stabilization or ligand field stabilization effects.[1,2] It can also switch from four to five or six coordination without considerable energy changes, making it highly suitable for enzyme active sites, where the mobility of coordinating amino acids is restricted.[3] Zinc is the second most abundant transition metal in the body, with the average human being composed of 2–3 g.[4] It is employed as a required cofactor that can stimulate the activities of approximately 300 enzymes.[5–9] It is necessary for DNA synthesis[6] and instrumental to growth and development from conception.

However, too much can be harmful,[9] because zinc is associated with several cytotoxic reactions. Abnormal zinc metabolism is associated with many health problems, ranging from superficial skin diseases to prostate cancer, diabetes and brain diseases. There is about 0.1–0.5 mM of zinc in brain tissue, higher than in any other organ.[10] A large amount of zinc accumulates in nerve cells, where the level of ionic Zn(II) is tightly regulated by zinc transport proteins[11] and metallothioniens.[12] Variations from these requirements are detrimental to cell survival. Abnormal zinc content has been reported to induce selective neural cell death associated with several acute conditions, including epilepsy, transient global ischemia, brain injury and chronic problems such as Alzheimer's, Parkinson's and Wilson's diseases, amyotropic lateral scelerosis (ALS) and some diseases caused by prions.[13–22]

Since zinc is so important, imaging zinc, especially so-called "free zinc", is becoming crucial to the elucidation of zinc concentration, distribution, kinetics and functions in cells and tissues.[23] For *in vivo* imaging, a sensitive and non-invasive technique is desirable in order to accomplish real-time local imaging. Different from other transition metal ions such as Fe(II), Mn(II) or Cu(II), Zn(II) does not give many spectroscopic signals due to its $3d^{10}4s^0$ configuration. Common

[a] *Department of Chemistry and Physical Sciences, Pace University, New York, NY 10038, USA. E-mail: zdai@pace.edu*
[b] *Department of Chemistry, New York University, New York, NY 10003, USA. E-mail: james.canary@nyu.edu*

Zhaohua Dai obtained his BS in 1996 from Wuhan University, which is located in the capital city of his home province of Hubei in central China. After gaining his MS in 1999 from the Chinese Academy of Sciences in Beijing, he was admitted to New York University, where he received his PhD in chemistry in 2004. After a postdoctoral stint with Professor David S. Lawrence at Albert Einstein College of Medicine, he joined Pace University as an assistant professor in January 2006. His research interests include the development of sensing systems for analytes of environmental, biological and forensic importance.

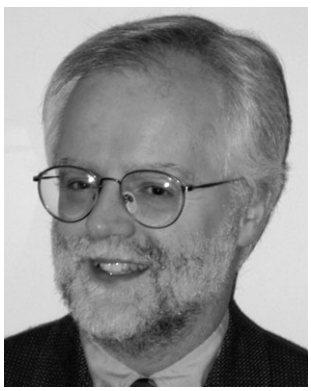

James W. Canary is a native of northwestern Nevada, where he began his undergraduate studies at the University of Nevada, Reno. He finished his BS degree at the University of California, Berkeley. He received his PhD under the direction of Donald Cram at the University of California at Los Angeles. In 1991, after completing an NIH postdoctoral fellowship with Ronald Breslow at Columbia University, he joined the New York University faculty. Professor Canary's work and interests span a wide range; from chiroptical spectroscopy to nucleic acid-templated polymer assembly to biomedical imaging.

spectral techniques such as UV-vis cannot be used. Nuclear magnetic resonance (NMR) is possible but limited by sensitivity and resolution, in part due to the nuclear quadrupole moment of Zn(II).[24–26] There have been efforts to develop contrast agents that might enable the MRI imaging of Zn.[27] Some methods, such as sulfide–Ag staining,[28] atomic absorption spectrometry, synchrotron radiation X-ray (SRXRF) spectrometry[29] and microparticle-induced X-ray emission (micro-PIXE),[30] are demanding of special instrumentation or may be suitable for few biological applications. Fluorescent sensors for zinc have been studied intensively recently because of their high sensitivity. Several reviews on fluorescent sensors for zinc have appeared.[23,31–38] However, the vast majority of known fluorescent sensors only produce intensity changes in emission upon exposure to zinc ions. This review highlights recent advances in the development of tripodal compounds as zinc sensors, especially our work in the field of sensing "invisible" Zn(II) using steady-state fluorescence, fluorescence lifetimes and chiroptical spectroscopy. Our approach has emphasized creative ligand design and detection schemes. Also included are results with tripodal ligands that have focused more on applications.

Tripodal ligands

Small molecule coordination systems are becoming increasingly important in supramolecular chemistry and molecular recognition. Among them, tripodal ligands have attracted considerable interest. A tripodal ligand is characterized as a compound with three coordinating arms. Typically, each of these arms has one or more donor atoms (N, O, S, P) connected to an anchoring nitrogen or phosphorous atom by two or three carbons.[39] The pendant coordinating arms may contain amino, pyridyl, quinolyl, carboxyl, alkoxyl, thioether and phosphoryl moieties, among others. Tripodal ligands may also provide an approach for metal sensing by fluorescence. Several recently reported zinc sensors, developed by several research groups, have a dipicolyl amine (DPA) fragment.[40–51] Some tripodal ligands based on its tripodal cousin tris-(2-pyridylmethyl)amine (TPA, Scheme 1), which possesses four nitrogen atoms for the ligation of a wide variety of metal ions, have been prepared in this lab and by others.[52–63] Applications of TPA-based tripodal complexes include metalloprotein models,[64,65] catalysis and [66,67] molecular recognition.[55,68]

One advantage of using chiral tripodal ligands for metal sensing is that they form complexes with metal ions of a defined configuration. For example, TPA (Scheme 1) forms propeller-shaped complexes with transition metal ions such as Cu(II) and Zn(II). As is shown in Fig. 1, the propeller can adopt both left- and right-handed C_3 or achiral C_σ configurations.[54,58] However, when a methylene proton is substituted with a methyl to give α-MeTPA (Scheme 1), the *S*-isomer predominantly forms a right-handed propeller with metal ions,

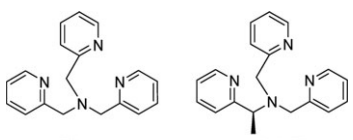

Scheme 1 Structures of TPA and α-MeTPA.

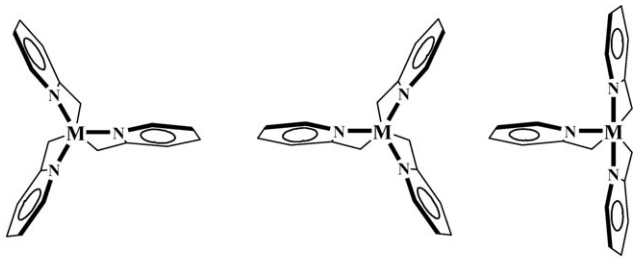

(**a**) C_3, right-handed, Δ (**b**) C_3, left-handed, Λ (**c**) C_σ, achiral

Fig. 1 Possible conformations of TPA, as found in various metal complexes.[54] Reprinted with permission from the American Chemical Society.

and the *R*-isomer predominantly forms a left-handed propeller (Fig. 2). It was found by calculation that there is a 1–2 kcal mol^{-1} preference for the *anti*-conformation. The relationship between the absolute configuration of the carbon center dictates the handedness of the propeller twist, as observed generally in computations and various structural data for these complexes, including crystallographic structures.[69] Therefore, the chirality of ligands can be harnessed to control the configuration of metal complexes.

Another advantage of chiral ligands is that they can yield additional spectroscopic information. Their chiral complexes can yield extra information from NMR, polarimetry, optical rotary dispersion (ORD) and circular dichroism (CD) measurements. Chiral tripodal TPA analogs can offer another powerful tool, exciton-coupled circular dichroism (ECCD),[57,69–71] whose signal is characteristically bisignate and generally much stronger than induced CD. The bisignate signal consists of a positive first cotton effect and a negative second Cotton effect, with a strong amplitude if the transition moments are arranged in a clockwise orientation, as shown in Fig. 2. The opposite applies if the transition moments are arranged in a counterclockwise orientation. Consideration of the potential chiroptical properties of chiral tripodal ligands opens up the possibility of developing new analytical methods to improve sensitivity or contrast.

Tripodal zinc sensors

High zinc sensitivity

Zinc sensors may find a variety of applications. For example, sensors of image free or vesicular zinc should display

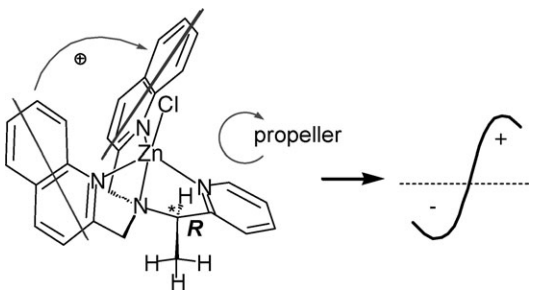

Fig. 2 Left-handed propeller (clockwise orientation of quinoline transition dipoles) gives rise to a positive couplet in ECCD.

association constants in the mM range.[23] On the other hand, probes with much higher affinities may be needed to probe phenomena where the metal is scarce or when competition with a protein receptor is desired.[72]

One advantage that tetradentate N_4 tripodal ligands offer as metal sensors is their overall strong binding properties. TPA binds strongly to both Zn(II) (log K = 11.0; K = [ML]/[M][L]) and Cu(II) (log K = 16.2) with a 1 : 1 stoichiometry.[73] Initially, a chiral ligand was studied, in which two of the pyridyl moieties were replaced with quinolyl groups[74] to make MeBQPA[55] (compound **1**, Scheme 2), whose fluorescence was enhanced by zinc binding (Fig. 3). Later, we constructed a series of compounds (Scheme 2)[75] containing 8-hydroxyquinoline (8-HQ), a well-known chromophore and an established analytical tool for zinc chelation.[76] By replacing the pyridyl ring with 8-HQ on two of the TPA arms, compound **2** was obtained. Introduction of dimethyl sulfonamide groups to each of the 8-hydroxyquinolines in compound **2** resulted in compound **3**, which showed an enhanced fluorescence quantum yield. Compound **4**, which has two picolyl arms instead of one, as in compound **3**, was also prepared. Compounds **2**, **3** and **4** exhibited enhanced fluorescence upon binding Zn(II) and a high affinity for zinc, with log K = 12.07, 13.07 and 14.34, respectively. Attachment of another dimethyl sulfonamide group to the chromophore of compound **4** resulted in compound **5**, which showed better fluorescence properties.[77] Compound **5** responds to Zn(II), with chelation-enhanced steady-state fluorescence properties showing sub-picomolar sensitivity (Fig. 4). The detection limit of **5** was from 10 fM to 1 pM (log K = 13.29). These highly chelating ligands were designed to display 1 : 1 M : L stoichiometry, as confirmed by the X-ray crystallographic structure of [Zn(**5**)] and strong sensitivity for Zn(II) (similar to or better than TPA). The mechanism of fluorescence enhancement is complex: 8-HQ compounds are poorly fluorescent (quantum yield Φ = 2%), in part due to photoinduced electron transfer (PET) involving the lone pair of the tertiary nitrogen and in part due to excited-state proton transfer (ESPT) caused by the phenolic proton and the nitrogen of 8-HQ.[78] Upon complexation of Zn(II), the lone pair of the tertiary nitrogen is coordinated to the metal, thereby eliminating PET. In addition, metal complexation results in the loss of the phenolic proton, eliminating ESPT. Aggregation also plays a role in the fluorescence enhancement mechanism.

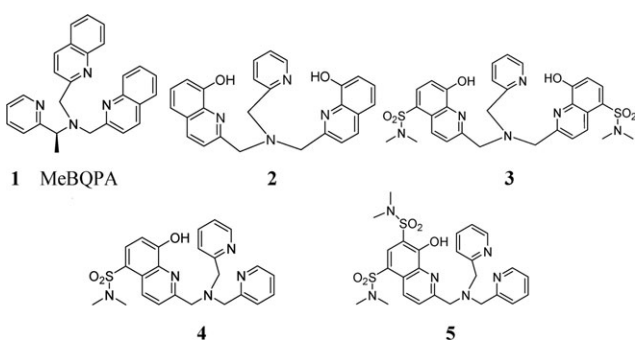

Scheme 2 Quinoline- and 8-hydroxyquinoline-based tripodal Zn(II) sensors.

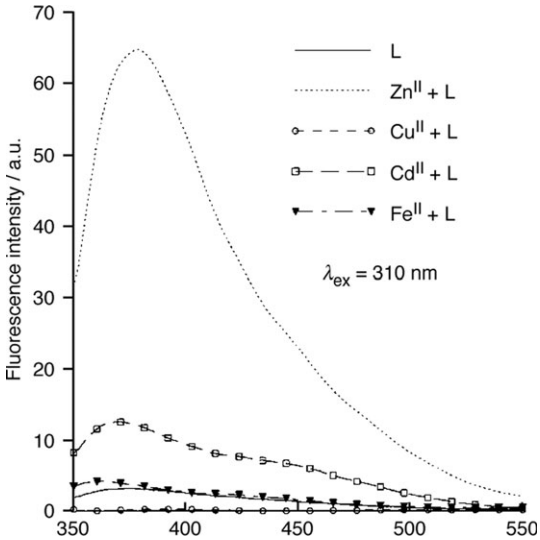

Fig. 3 Fluorescence spectra of MeBQPA and complexes with $Zn(ClO_4)_2$, $Cd(NO_3)_2$, $Cu(ClO_4)_2$ and $FeCl_2$ in aqueous HEPES buffer at pH 7.09. Adapted from ref. 55.

Improved Zn(II)/Cu(II) selectivity

One issue that haunts analyte recognition is interference by other metal ions. Many reported fluorescent chemosensors for Zn(II) suffer from interference by the binding of Cu(II),[45,79] which commonly forms more stable complexes than Zn(II) with many ligands.[43,80,81] For example, recognition of Zn(II) by compound **1** benefited from both fluorescence enhancement as well as chiroptical signal increase. However, Cu(II) was a significant competitor for Zn(II) in that system.[55]

Modulation of achiral metal ion behavior by the stereocontrol of organic ligands is not without precedence.[82–86] A combination of ligand geometry and stereocontrolled substitution can lead to improved Ag^+ affinity in some podand ligands bearing pyridine moieties and two chiral arms.[60,87] Open chain TPA analogs with two chiral arms have been used to tune lanthanide luminescence.[62]

We have developed an approach to engineering improved Zn(II)/Cu(II) selectivity by controlling ligand stereochemistry.[88] The design of a selective ligand for a metal ion must

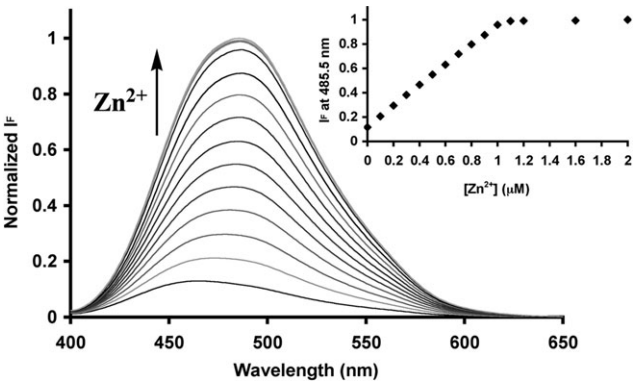

Fig. 4 Fluorescence enhancement of **5** as a function of Zn(II) concentration. Inset: Fluorescence as a function of added Zn(II) monitored at 485.5 nm.

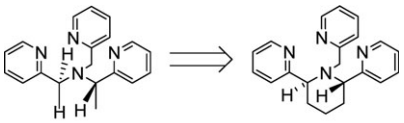

Scheme 3 Design of rigid chiral scaffolds.

involve a high degree of preorganization for the specific metal ion, and also a high degree of mismatch for competing metal ions. Due to its closed shell configuration, Zn(II), like Cu^+,[89] is not strongly influenced by constraints in its coordination configuration. Therefore, it is necessary to make a ligand that has a high degree of preorganization to mismatch Cu(II). As a d^9 metal, the bonding in Cu(II) complexes is partially covalent, and it prefers 4-coordinate square planar and 5-coordinate square pyramidal geometries to tetrahedral and trigonal bipyramidal geometries.[1] C_3 or pseudo-C_3 symmetrical N-containing TPA derivatives bind Cu(II) much better than Zn(II), as predicted by the Irving–Williams series.[89] At the same time, their conformational behavior naturally favor metal ions with a trigonal bipyramidal geometry. To accommodate Cu(II), this trigonal bipyramidal configuration is often distorted to resemble a square pyramidal geometry. However, we can construct tripodal ligands that are incapable of adapting to a planar geometry but could readily accommodate tetrahedral or distorted tetrahedral geometries.[90]

To improve the Zn(II)/Cu(II) selectivity of TPA-based sensors, our strategy was to impose a trigonal bipyramidal coordination geometry. Rigidification is a common approach to preorganization, and, in principle, it should also work to preorganize towards a mismatch. To achieve this, a ring was incorporated into the TPA ligand by connecting two of the arms. As shown in Scheme 3, this gave a piperidine scaffold. The piperidine ligand would require identical stereochemistry at the two chiral centers to enforce a C_3 coordination environment. The piperidine would also reduce conformational mobility by rigidifying the compound. A similar rationale was used to design ligands that stabilize Cu(I) over Cu(II).[90]

Initially, compounds without chromophores, **6** and **7** (Scheme 4), were prepared and examined for their binding ability and characterized to verify the structural hypothesis.[88,91] For the *cis*-piperidine derivative **6**, Cu(II) and Zn(II) gave log β = 14.8 and 10.1, respectively, and for *trans*-ligand **7**, the corresponding values were found to be 12.0 and 11.2, respectively. The parent compound TPA shows log β = 16.15 for Cu(II) compared to 11.00 for Zn(II).[12] Thus, the ratio of the association constants for the binding of Cu(II) over Zn(II) for TPA, **6** and **7** is 1.4×10^5, 5×10^4 and 6, respectively. While *cis*-ligand **6** showed diminished binding for both Cu(II) and Zn(II), *trans*-ligand **7** showed even poorer binding of Cu(II) but a slightly stronger binding of Zn(II) over TPA.

The results of PM3/tm calculations agree with the observation that the binding of Zn(II) is little dependent on ligand stereochemistry, while for Cu(II), ligand **6** is preferred significantly. The computed structures and X-ray structures show greater similarity of the $[Cu(TPA)Cl]^+$ Cu–N bond lengths in complex **6** than in **7**. Thus, *trans*-ligand **7** appears to distort the coordination sphere of the Cu ion, resulting in a less stable complex.

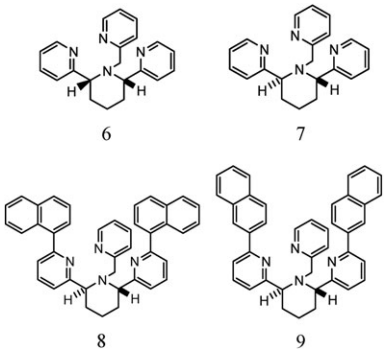

Scheme 4 Rigidified tripodal ligands.

Subsequently, *trans*-ligand **7** was tagged with naphthalene fluorophores to prepare ligands **8**[88] and **9**[92,93] (Scheme 4). The fluorescence of the naphthalene moieties is diminished by PET in the absence of a metal ion, but increases nearly 20-fold upon binding Zn(II) for compound **8**. The sensitivity of compound **8** for Zn(II) was found to be nM in HEPES buffer with 1% methanol at physiological pH. As expected, based on the studies of **6** and **7**, Cu(II) competed with Zn(II) for **8** and **9**, resulting in the quenching of fluorescence by energy transfer between the paramagnetic metal ion and fluorophore. Other biologically relevant metal ions have little or no influence on their sensing properties. The improved selectivity found for ligand **7** was also observed with compounds **8** and **9**. The binding constants and metal selectivity of these compounds to Cu(II) and Zn(II) are compiled in Table 1. Thus, stereochemical engineering of ligands by constructing an unfriendly environment for Cu(II) to depress Cu(II) affinity and enhance Zn(II)/Cu(II) selectivity has proved to be feasible.

Chiroptical tripodal sensors

Aside from stereochemical control, another advantage of chiral ligands is that they can yield additional spectroscopic information. Using chiral ligands, we have developed a sensing strategy wherein both isotropic and anisotropic absorption signals from the optical response of a single sensory molecule provide not only detection but also differentiation of multiple analytes. Zinc greatly enhances the fluorescence of ligand **1**, α-MeBQPA.[55] However, its fluorescence responses to other metal ions are different. The ligand also generates strong signals in the ECCD upon formation of complexes with some metal ions (Zn(II), Cu(II)), while complexes with octahedral metal ions (Cd(II), Fe(II)) do not give strong CD signals (Fig. 5). The fluorescence and ECCD properties of the complexes result in the interesting situation that the ligand can not only signal the presence of a metal ion, but evaluation of both

Table 1 Binding constants and Zn(II)/Cu(II) selectivity of ligands **8** and **9** in 15% acetonitrile 50 mM HEPES buffer (0.1 M KNO_3, pH 7.19)

Compound	log K_{ZnL}	log K_{CuL}	K_{ZnL}/K_{CuL}	K_{ZnL}/K_{CuL} by competition experiment
8	7.44	7.64	0.64	0.5
9	7.08	7.06	1.04	N/A

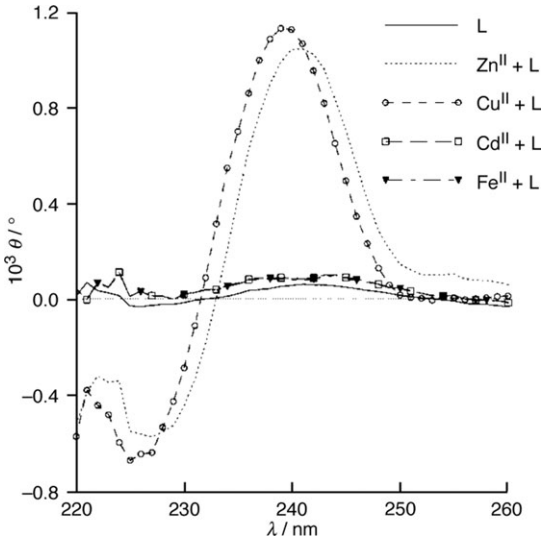

Fig. 5 CD spectra of (*R*)-α-MeBQPA and its complexes with $Zn(ClO_4)_2$, $Cd(NO_3)_2$, $Cu(ClO_4)_2$ and $FeCl_2$ in aqueous HEPES buffer at pH 7.09. Adapted from ref. 55.

properties can allow identification of the metal. As illustrated in Fig. 6, detection of both fluorescence enhancement and anisotropic absorption distinguishes Zn(II) (strong fluorescence and ECCD response) from other metal such as Cu(II) (strong ECCD but no fluorescence), Cd(II) (strong fluorescence but no ECCD) and Fe(II) (neither fluorescence nor ECCD).

Our interest in chiroptical materials also led us to examine a new approach to metal ion sensing using fluorescence-detected circular dichroic detection (FDCD), which integrates fluorescence and exciton coupled circular dichroism methods to give a better contrast than those that can be achieved in either of the two parent methods.[93] Typically, the two channels of raw FDCD data, which correspond to the difference in emission ($F_L - F_R$; F_L, F_R = fluorescence with left and right circularly polarized excitation, respectively) and the total emission ($F_L + F_R$) resulting from differential absorption of left- and right-circularly polarized light, are converted to a CD spectrum by established methods. An adaptation of the FDCD technique can provide a unique and powerful new strategy for sensor applications by using the ΔF ($\Delta F = F_L - F_R$)[94] component of the FDCD data directly, without conversion to CD. This new method was named differential circularly polarized fluorescence excitation (CPE) to distinguish it from

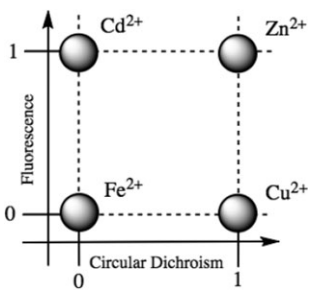

Fig. 6 Chiroptically-enhanced fluorescence detection of Zn(II) by compound **1**.

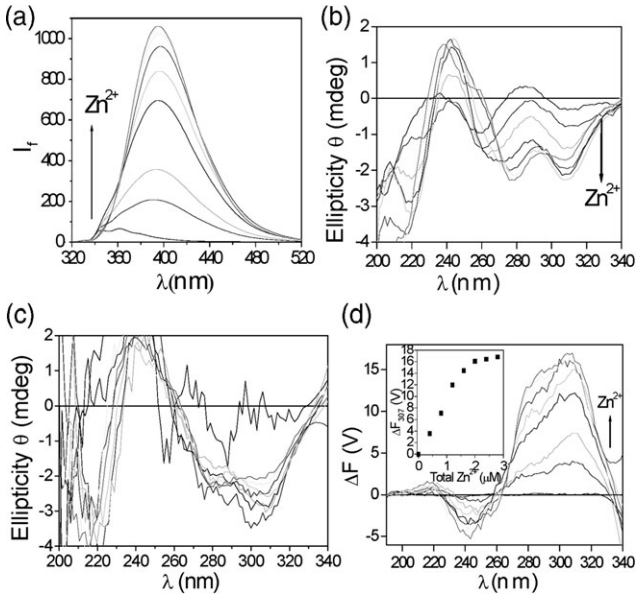

Fig. 7 Spectral response of 2 μM (*S*,*S*)-**2** to Zn(II) in acetonitrile: (a) Fluorescence (ex.: 300 nm), (b) CD, (c) FDCD and (d) ΔF (inset: titration curve of 2 μM (*S*,*S*)-9 with $Zn(ClO_4)_2$).[93] Reprinted with permission from the American Chemical Society.

traditional FDCD. Materials with higher ellipticity, θ, and higher fluorescence quantum yield, Φ_F, will lead to an even larger ΔF. Substances lacking either fluorescence or CD properties will not be observed. The contrast in the ΔF signal between a sample with both a large quantum yield and large CD, and a sample with both a small quantum yield and small CD will be much larger than the contrast in either fluorescence or CD signals. We compared the fluorescence, CD, UV and ΔF spectra of ligands **8**, **9**, **10** and their enantiomers. The corresponding spectra of compound **9** [(*S*,*S*) form], titrated with Zn(II), are shown in Fig. 7. The maximum observed enhancements after the addition of 1 equivalent of zinc (fluorescence quantum yield, fluorescence maxima value, CD ellipticity at 307 nm and ΔF value) are compiled in Table 2. Apparently, measurements of ΔF gave greatly enhanced contrast. Traditional FDCD (Fig. 7(c)) and $\Delta F/F$ do not offer such advantages because they cancel out the contribution from fluorescence.

The CPE approach has the potential to improve contrast and diminish interference from background fluorescence in zinc sensing. ΔF titrations of (*R*,*R*)-**9** with zinc in the presence of 1.0 mg mL^{-1} lysozyme (Fig. 8), which contains several tryptophan residues, a common source of background fluorescence in cells, showed excellent contrast and linearity, while

Table 2 Contrast in Zn(II) binding in acetonitrile

	8	**9**
Φ_L	0.003	0.009
Φ_{ML}	0.176	0.170
Φ_{ML}/Φ_L	55	19
F_{ML}^{max}/F_L^{max}	90	16
$\theta_{ML}^{307}/\theta_L^{307}$	4.5	6.4
$\Delta F_{ML}^{307}/\Delta F_{ML}^{307}$	>500	>200

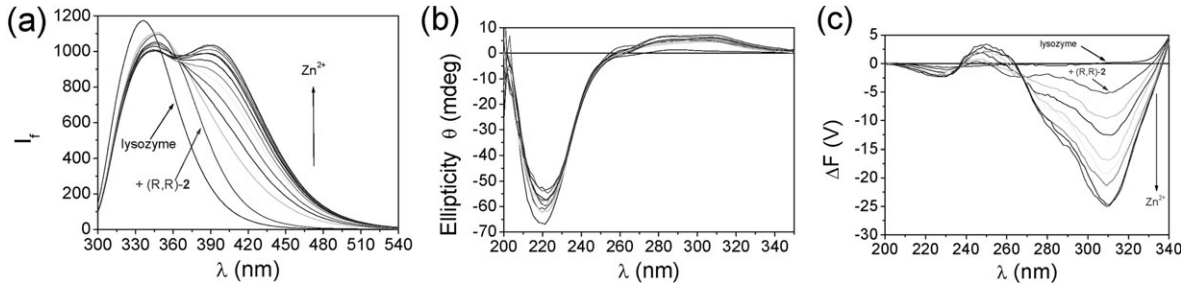

Fig. 8 Spectral responses of 3.2 μM (*R*,*R*)-**9** to Zn(II) in the presence of 1.0 mg mL^{-1} HEW lysozyme in 60% acetonitrile/water: (a) Fluorescence (ex.: 280 nm), (b) CD and (c) ΔF.[93] Reprinted with permission from the American Chemical Society.

fluorescence, UV and CD measurements were significantly obscured by the background signals from the protein. These results lay the groundwork for the development of imaging tools for use in conjunction with isotropic fluorescence and CD microscopy,[94] potentially offering better contrast and unique advantages, such as turbid solution analysis. Systems with more practical chromophores would enhance the applicability of this method.

Ratiometric time-resolved fluorescence sensor for Zn(II)

Ratiometric agents are highly desirable because of the ability to visualize both ligand and metal concentration.[48,95–97] Wavelength ratiometric agents display different fluorescence emission maxima for the ligand and its metal complex. The potential advantage of this approach is ready visualization by color, although quantification invariably requires digitization and processing of the data. We have developed a novel and sensitive probe for the ratiometric detection of Zn(II) utilizing time-resolved fluorescence (TRF) techniques that provide invaluable information about a system when multiple fluorescence-emitting components are contributing to its steady-state fluorescence intensity.[77] Using time domain TRF techniques, a marked improvement over steady-state fluorescence methods for the ratiometric detection of Zn(II) was achieved using novel ligand **5** (Scheme 2). The fluorescence intensity $I(t)$, which is a function of time, at different Zn(II) concentrations depends on the lifetime values of the free ligand and its Zn(II) complex (τ_f and τ_{Zn}, respectively). Steady-state fluorescence measurements cannot ascertain whether the two-state model is applicable. On the other hand, the contributions of each component, $A_f\tau_f$ and $A_{Zn}\tau_{Zn}$, can be determined separately by TRF methods. A_f and A_{Zn} are fractions that are proportional to $\varepsilon_f c_f$ and $\varepsilon_{Zn} c_{Zn}$, where c_f and c_{Zn} are the concentrations of the free and Zn-bound molecules, and ε_f and ε_{Zn} are the molar extinction coefficients of free and Zn-bound ligand. For compound **5**, the $I(t)$ signal decays rapidly in the absence of Zn(II), with a dominant component with $\tau_f(1) = 0.64$ ns, $A_f(1) = 0.96$, and a minor second component with $\tau_f(2) = 24.9$ ns, $A_f(2) = 0.044$. The contribution of the slower fluorescence component gradually increases as the concentration of Zn(II) is increased (Fig. 9). Excellent ratiometric behavior was observed (Fig. 9, inset). The dynamic range of TRF is significantly larger than that of steady-state fluorescence spectral measurements. Strong differences in fluorescence lifetimes were observed in live cells incubated in a solution of **5**. The selectivity of **5** for Zn(II) and the time-resolved fluorescence data not only allow the accurate detection of this ion, but also allow discrimination between other fluorescent forms of the probe and its metal complexes.

Other tripodal zinc sensors

Although this review has focused on research in our own laboratories, a number of other research groups have also recognized the utility of tripodal scaffolds for the development of zinc sensors. For example, fluorescein has been derivatized with a DPA (di-2-picolylamine) fragment, a binding moiety structurally similar to TPEN (*N*,*N*,*N*,*N*-tetra(2-picolyl)ethylenediamine), which is a membrane permanent heavy metal chelator with a high affinity. Replacing the pyridyl rings in this compound with quinolyl rings led to the formation of TQEN (*N*,*N*,*N*,*N*-tetra(2-quinolylmethyl)ethylenediamine). TQEN and its derivatives have been used as fluorescent zinc sensors.[98] Newport Green (Scheme 5), a commercially available sensor that falls into this category, is cell-impermeable. It exhibits a 3.3-fold enhancement upon binding 1 equivalent of Zn(II) under physiological conditions. It has a moderate zinc binding affinity (K_d for Zn(II) ~ 1 μM), but is essentially insensitive to Ca(II) (K_d for Ca(II) > 100 μM).[99] Lippard's Zinpyr (ZP, Scheme 5)[33,40,45,46,51,100–102] and derivatives (Scheme 6),[44,48,103,104] Zinspy (ZS, Scheme 7)[79,105] and Nagano's ZnAF (Scheme 8)[41–43,49] families are more recent examples of this class of sensors with improved properties. Since a

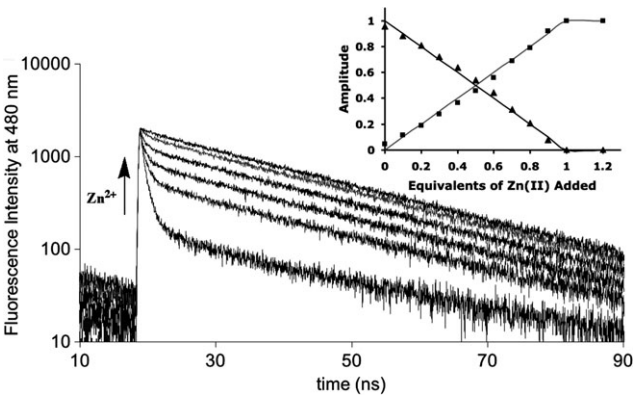

Fig. 9 Exponential fluorescence decays as a function of Zn(II) concentration measured at 480 nm. Spectra inset: A_f (▲) and A_{Zn} (■) as a function of Zn(II) concentration.[77] Reprinted with permission from the American Chemical Society.

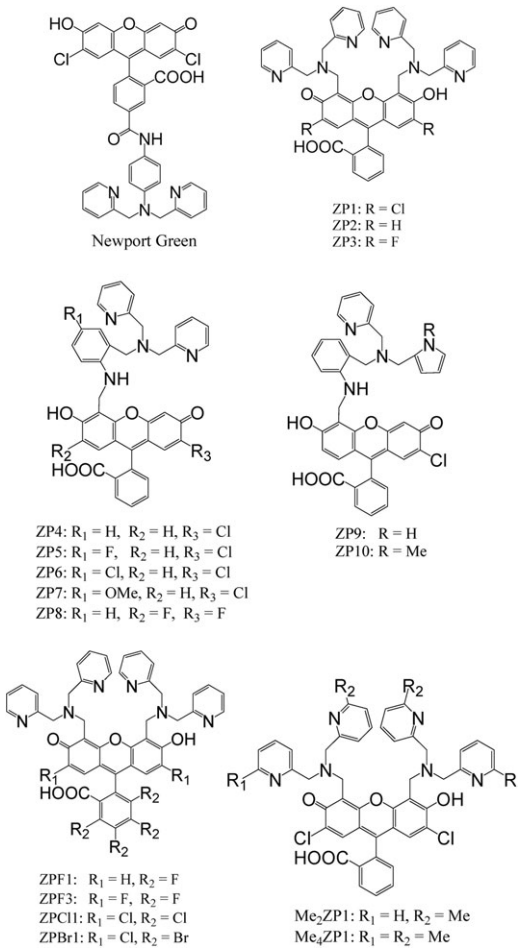

Scheme 5 Structure of Newport Green and the Zinpyr (ZP) family sensors.

heteroatom on the third arm participates in binding zinc in many of these sensors, they are tripodal ligands.

The Zinpyr sensors (Scheme 5) are selective for Zn(II) over Ca(II) and Mg(II). Both cell-permeable and cell-impermeable forms are available,[106] depending on the application requirements. The Zinpyr family are better choices than the TSQ family of sensors for imaging the vesicular pool of Zn(II).[23] They are stable under physiological conditions, remain in vesicles and have been used to image brain slices by confocal microscopy. ZP1 has a low nM affinity for Zn(II).[40,51] Replacing two or four pyridyl groups in ZP1 with 6-methylpyridyl groups results in new sensors Me_2ZP1 and Me_4ZP1 (Scheme 7),[102] respectively. Upon binding 1 equivalent of Zn(II), there

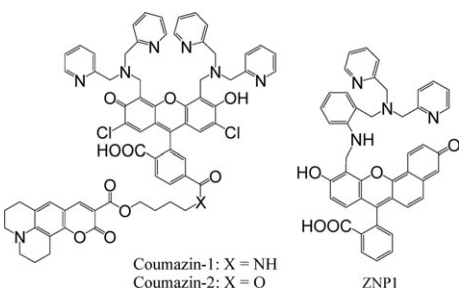

Scheme 6 Structures of Zinpyr derivatives.

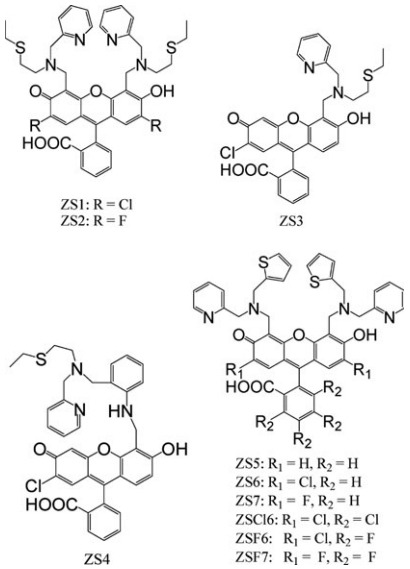

Scheme 7 Structures of the Zinspy (ZS) family sensors.

were 4-fold and 2.5-fold increases in fluorescence emission for Me_2ZP1 and Me_4ZP1, respectively. Substituting one of the picolyl groups in ZP1 with an alkyl group results in Zin-AlkylPyr (ZAP)[107] analogues ZAP1 or ZAP2 (if the substitution was methyl) and ZAP3 (if the substitution was benzyl) (structures not shown). These probes provided insights into the importance of pH-dependent background emission and other structural parameters in the system.

As a membrane-impermeable probe, ZP4 is a second generation version of ZP1.[45] When ZP4 was exposed to 1 equivalent of Zn(II), there was a 5-fold enhancement in fluorescence. The dissociation constant of the ZP4-Zn(II) complex was around 0.6 nM. When one of the pyridyl groups in ZP4 was replaced with a pyrrole or *N*-methylpyrrole, ZP9 or ZP10 was obtained.[101] ZP9 gave 12-fold and ZP10 gave 7-fold enhancements when complexed with Zn(II). They showed a mid-range affinity for Zn(II), with sensitivities in the sub-micromolar range (0.69 μM) for ZP9 and low-micromolar range (1.9 μM) for ZP10.

The fluorescence properties of ZP1–7 and ZP9–10 are pH-dependent, with or without Zn(II). By introducing fluorine onto the fluorescein backbone and by the substitution of an aliphatic nitrogen with an aniline nitrogen, improved pH-dependent properties and dynamic range were obtained for ZP8,[100] which has been used in the two-photon microscopy detection of endogenous Zn(II) pools.

Lippard *et al.* fabricated Coumazin-1 and Coumazin-2 (Scheme 6), by functionalizing ZP1 with a Zn-insensitive fluorophore, coumarin 343.[48,103] This system was used for ratiometric zinc sensing based on the esterase-mediated cleavage of the sensor into two separate parts: the coumarin and the zinc sensor ZP1. Coumarin 343 emission revealed the sensor concentration and ZP1 emission revealed the relative concentration of Zn(II)-bound sensor.

The Lippard group made another intracellular fluorescent probe, Zin-naphthopyr-1 (ZNP1)[104] (Scheme 6), which is similar to the Zinpyr family. The sensor enables single-excitation, dual-emission, ratiometric detection of Zn(II) through the

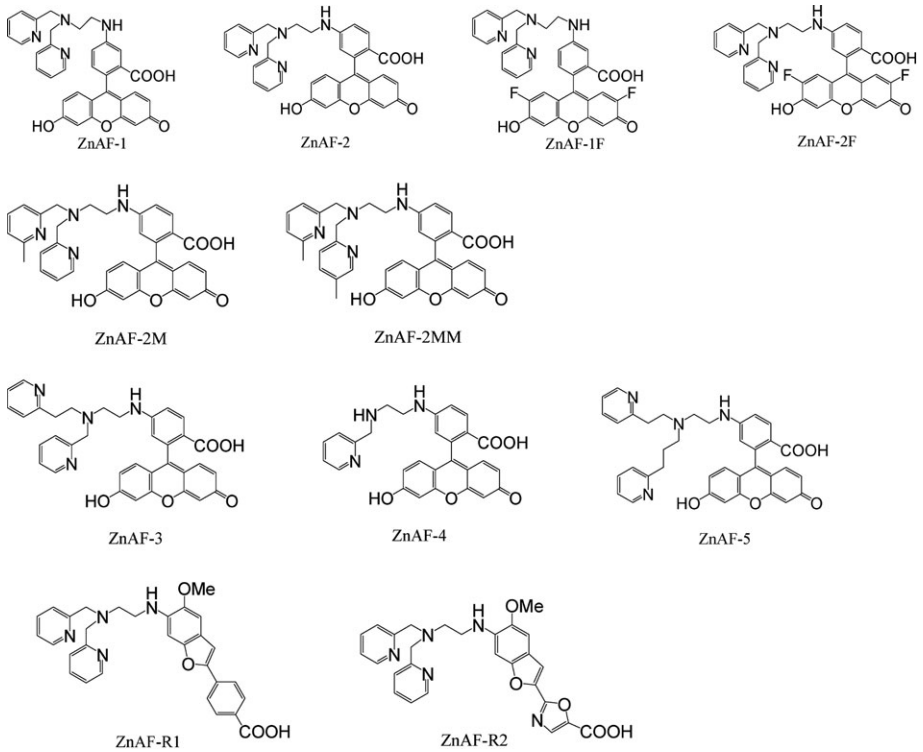

Scheme 8 Structures of the ZnAF family sensors.

chromophore switching between its fluorescein and aphthofluorescein tautomeric forms, a process controlled by Zn(II). It offers an 18-fold increase in fluorescence emission intensity ratio ($\lambda_{624}/\lambda_{528}$) upon zinc binding.

The Zinpyr sensors' dissociation constants for Zn(II) are in the nM range.[45,46] As previously mentioned, some applications require a lower affinity. To modulate Zn affinity and improve the selectivity over other first-row transition metal ions, thioethers were used to substitute one or two pyridyl groups in the Zinpyr structure to give Zinspy (ZS) sensors (Scheme 7) ZS1–4.[79] These ZS probes exhibit improved Zn(II) selectivity and tunable affinity for Zn(II), but the fluorescence properties are not as favorable when compared to the Zinpyr family. Thiophene moieties were used to substitute the thioether(s) in ZS1–4 to construct other Zinspy sensors (ZS5, ZS6, ZS7, ZSCl6, ZSF6, ZSF7),[105] giving enhanced fluorescence properties, low-micromolar dissociation constants for Zn(II) and improved Zn(II) selectivity, especially over mercury (however, these ligands do not behave as tripodal ligands, since thiophene does not coordinate to Zn(II)). Lippard's recent quinoline and fluorescein-based zinc sensors, QZ1 and QZ2,[108] show an outstanding dynamic range and fluorescence enhancement, although they are not tripodal ligands.

Halogenation of the xanthenone and benzoate moieties of the fluorescein platform systematically modulates the photophysical and complexation properties of Zinpyr and Zinspy sensors.[79,100] Nagano *et al.* adopted a similar approach by turning ZnAF-1 and ZnAF-2 into better Zn probes ZnAF-1F and ZnAF-2F, respectively (Scheme 8).[43] The fluorescence intensity of ZnAF-1 and ZnAF-2 increased to 17-fold and 51-fold,[42] respectively, upon addition of 1 equivalent of Zn(II) at pH 7.5. ZnAF-2 has been immobilized onto a glass slide to probe zinc ion release from pancreatic cells.[109] However, under acidic conditions (the pK_a values for ZnAF-1 and AF-2 are both 6.2), the enhancement is not as impressive. Incorporation of fluorine into the fluorescein platform produces ZnAF-1F and ZnAF-2F, shifting their pK_a to 4.9.[43] Upon binding 1 equivalent of Zn(II) at pH 7.4, their fluorescence is enhanced by 69- and 60-fold, respectively.

Thus, ZnAF-1F and ZnAF-2F are excellent Zn sensors in neutral and slightly acidic conditions. Their fluorescence properties are independent of pH over a much wider range than ZnAFs, and are therefore more suitable in applications where the pH varies. Diacetyl derivatives of these sensors are cell-permeable. Other similar sensors were reported by Nagano's group.[49] These sensors have shown a wide range of affinities for Zn, with the following dissociation constants: ZnAF-1 0.78 nM, ZnAF-2 2.7 nM, ZnAF-1F 2.2 nM, ZnAF-2F 5.5 nM, ZnAF-2M 38 nM, ZnAF-2MM 3.9 μM, ZnAF-3 0.79 μM, ZnAF-4 25 μM and ZnAF-5 0.60 mM. Therefore, a wide Zn(II) concentration range from 10^{-10} to 10^{-3} M can be monitored by using different sensor molecules or combinations.

Utilizing benzofuran derivatives as the fluorophores, the Nagano group fabricated ZnAF-R1 and ZnAF-R2.[110] ZnAF-R2 is more water-soluble and more fluorescent than ZnAF-R1. Although Zn(II) decreased the fluorescence intensity, there was a blue-shift in the excitation maximum. ZnAF-R2 is a membrane-permeable and ratiometric Zn(II) sensor with a high sensitivity against Ca(II), Na(I), Mg(II) and K(I).

Nagano also fabricated another DPA-based Zn(II) sensor (Scheme 9), in which two DPA moieties were connected together with a polyamine chain bearing lanthanide-binding

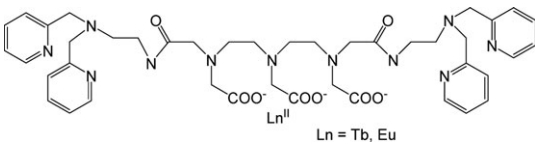

Scheme 9 Nagano *et al.*'s DPA–lanthanide-based Zn(II) sensor.

carboxyl side chains.[111] Before binding Zn(II), the lanthanide did not fluoresce when the system was irradiated at 260 nm. Zinc binding induced conformational changes, such that the energy absorbed by the pyridines could transfer to the lanthanide, and the system responded by lanthanide fluorescence. The system functioned at a 100 μM concentration level. The Gd(III) complex of this sensor has been used as a MRI contrast agent for the selective imaging of Zn(II).[27]

Conclusions and future perspective

There has been tremendous interest in detecting Zn(II), and many approaches have been reported. We have focused on developing chemistry that allows new strategies for sensing Zn(II). Utilizing TPA-based N_4 tripodal ligands has provided a flexible system for engineering zinc sensors with improved sensitivity, selectivity and contrast. Incorporating 8-HQ moieties into tripodal compounds increased their affinities for Zn(II). Using time domain TRF techniques, a marked improvement over steady-state fluorescence methods was achieved for the ratiometric detection of Zn(II): the data not only allowed for the accurate detection of this ion over a wider dynamic range, but also could discriminate between other fluorescent forms of the probe and its metal complex. Using chiral tripodal ligands not only enabled stereochemical control to achieve higher Zn(II)/Cu(II) selectivity, but also made it possible to extract both isotropic and anisotropic absorption signals from the optical response of a single sensory molecule. Chiroptical methods, including CPE, provide not only detection but also the differentiation of multiple analytes. The CPE approach can help to greatly enhance sensing contrast, diminishing interference from background fluorescence. The unique characteristics of ΔF augment the tool box of optical methods available for solution probes of metal ion binding, and the recognition and detection of other organic material. These results lay the groundwork for the development of imaging tools to be used in conjunction with isotropic fluorescence and CD microscopy,[112] potentially offering better contrast and unique advantages, such as turbid solution analysis. In addition to studies from our own laboratories, a wide variety of tripodal zinc sensors have been reported by others, displaying many novel features and finding application in biological studies.

From a broad perspective, many zinc sensors have now been described in the literature with a variety of properties. Certainly, there are many more bases to be covered. It seems likely that the most strategic progress, from an analytical point of view, is currently being made by chemists working with biologists on real life problems where the determination of zinc is required. Many of the lessons learned from zinc sensor research can be applied to the detection of other analytes. There is much interest in methods that can be used in living organisms; for example, 2-photon fluorescence methods may extend the utility of fluorescence to *in vivo* applications.[97,110] One exciting recent direction is the detection of zinc by methods that can be used *in vivo*, such as magnetic resonance imaging,[113,114] which could open up new biological research and human health opportunities. It is our opinion that fundamental chemical advances leading to new and different strategies for zinc detection should be encouraged, along side practical sensor development.

Acknowledgements

We gratefully acknowledge support from NSF (CHE-0316589, CTS-0608889) and NIGMS (grant GM-076202). Zhaohua Dai is grateful for support from Pace University.

References

1 F. A. Cotton, G. Wilkinson and P. Gaus, *Basic Inorganic Chemistry*, Wiley, New York, 1995.
2 A. E. Martell and R. D. Hancock, *Metal Complexes in Aqueous Solutions*, Plenum Press, New York, 1996.
3 B. L. Vallee and D. S. Anuld, *Acc. Chem. Res.*, 1993, **26**, 543–551.
4 F. A. Cotton and G. Wilkinson, *Advanced Inorganic Chemistry*, Wiley, New York, 1988.
5 L. A. Finney and T. V. O'Halloran, *Science*, 2003, **300**, 931–936.
6 D. P. Giedroc, K. M. Keating, C. T. Martin, K. R. Williams and J. E. Coleman, *J. Inorg. Biochem.*, 1986, **28**, 155–169.
7 A. S. Prasad, *Ann. Intern. Med.*, 1996, **125**, 142–144.
8 W. Maret, *BioMetals*, 2001, **14**, 187–190.
9 J. M. Berg and Y. Shi, *Science*, 1996, **271**, 1081–1085.
10 D. W. Choi, M. Yokoyama and J. Koh, *Neuroscience*, 1988, **24**, 67–79.
11 R. D. Palmiter, T. B. Cole, C. J. Quaife and S. D. Findley, *Proc. Natl. Acad. Sci. U. S. A.*, 1996, **93**, 14934–14939.
12 M. Ebadi, F. Perini, K. Mountjoy and J. S. Garvey, *J. Neurochem.*, 1996, **66**, 2121–2127.
13 R. J. P. Williams, in *Zinc in Human Biology*, ed. C. F. Mills, Springer-Verlag, London, 1989, pp. 15–31.
14 A. I. Bush, *Curr. Opin. Chem. Biol.*, 2000, **4**, 184–191.
15 A. Andrasi, E. Farkas, D. Gawlik, U. Rosick and P. Bratter, *J. Alzheimer's Dis.*, 2000, **2**, 17–26.
16 M. P. Cuajungco and G. J. Lees, *Neurobiol. Dis.*, 1997, **4**, 137–169.
17 M. P. Cuajungco and K. Y. Faget, *Brain Res. Rev.*, 2003, **41**, 44–56.
18 G. Faa, M. Lisci, M. P. Caria, R. Ambu, R. Sciot, V. M. Nurchi, R. Silvaqni, A. Diaz and G. Crisponi, *J. Trace Elem. Med. Biol.*, 2001, **15**, 155–160.
19 J.-Y. Koh, *Mol. Neurobiol.*, 2001, **24**, 99–106.
20 A. V. Kudrin and O. A. Gromova, *Trace Elem. Electrolytes*, 2003, **20**, 1–4.
21 S. W. Suh, K. B. Jensen, M. S. Jensen, D. S. Silva, P. J. Kesslak, G. Danscher and C. J. Frederickson, *Brain Res.*, 2000, **852**, 274–278.
22 N. T. Watt and N. M. Hooper, *Trends Biochem. Sci.*, 2003, **28**, 406–410.
23 C. J. Frederickson, *Sci. STKE*, 2003, pe18.
24 Y. Hang, S. Mukherjee and E. Oldfield, *J. Am. Chem. Soc.*, 2005, **127**, 2370–2371.
25 A. S. Lipton, T. A. Wright, M. K. Bowman, D. L. Reger and P. D. Ellis, *J. Am. Chem. Soc.*, 2002, **124**, 5850–5860.
26 A. S. Lipton, C. Bergquist, G. Parkin and P. D. Ellis, *J. Am. Chem. Soc.*, 2003, **125**, 3768–3772.
27 K. Hanaoka, K. Kikuchi, Y. Urano, M. Narazaki, T. Yokawa, S. Sakamoto, K. Yamaguchi and T. Nagano, *Chem. Biol.*, 2002, **9**, 1027–1032.

28 G. Danscher, S. Juhl, M. Stoltenberg, B. Krunderup, H. D. Schroder and A. Andreasen, *J. Histochem. Cytochem.*, 1997, **45**, 1503–1510.
29 R. Ishihara, Y. Kawakami, T. Takeuchi and A. Ide-Ektessabi, *Biomed. Res. Trace Elem.*, 2003, **14**, 204–209.
30 M. A. Lovell, J. D. Robertson, W. J. Teesdale, J. L. Campbell and W. R. Markesbery, *J. Neurol. Sci.*, 1998, **158**, 47–52.
31 P. Jiang and Z. Guo, *Coord. Chem. Rev.*, 2004, **248**, 205–229.
32 E. Kimura and T. Koike, *Chem. Soc. Rev.*, 1998, **27**, 179–184.
33 S. C. Burdette and S. J. Lippard, *Coord. Chem. Rev.*, 2001, **216–217**, 333–361.
34 S. C. Burdette and S. J. Lippard, *Proc. Natl. Acad. Sci. U. S. A.*, 2003, **100**, 3605–3610.
35 R. B. Thompson, *Curr. Opin. Chem. Biol.*, 2005, **9**, 526–532.
36 N. C. Lim, H. C. Freake and C. Bruckner, *Chem.–Eur. J.*, 2005, **11**, 38–49.
37 K. Kikuchi, K. Komatsu and T. Nagano, *Curr. Opin. Chem. Biol.*, 2004, **8**, 182–191.
38 E. Kimura and S. Aoki, *BioMetals*, 2001, **14**, 191–204.
39 H. Nagao, N. Komeda, M. Mukaida, M. Suzuki and K. Tanaka, *Inorg. Chem.*, 1996, **44**, 4756–4765.
40 S. C. Burdette, G. K. Walkup, B. Spingler, R. Y. Tsien and S. J. Lippard, *J. Am. Chem. Soc.*, 2001, **123**, 7831–7841.
41 T. Hirano, K. Kikuchi, Y. Urabo, T. Higuchi and T. Nagano, *Angew. Chem., Int. Ed.*, 2000, **39**, 1052–1054.
42 T. Hirano, K. Kikuchi, Y. Urano, T. Higuchi and T. Nagano, *J. Am. Chem. Soc.*, 2000, **122**, 12399–12400.
43 T. Hirano, K. Kikuchi, Y. Urano and T. Nagano, *J. Am. Chem. Soc.*, 2002, **124**, 6555–6562.
44 S. C. Burdette and S. J. Lippard, *Inorg. Chem.*, 2002, **41**, 6816–6823.
45 S. C. Burdette, C. J. Frederickson, W. Bu and S. J. Lippard, *J. Am. Chem. Soc.*, 2003, **125**, 1778–1787.
46 E. M. Nolan, S. C. Burdette, J. H. Harvey, S. A. Hilderbrand and S. J. Lippard, *Inorg. Chem.*, 2004, **43**, 2624–2635.
47 J. Yuasa and S. Fukuzumi, *J. Am. Chem. Soc.*, 2006, **128**, 15976–15977.
48 C. C. Woodroofe, A. C. Won and S. J. Lippard, *Inorg. Chem.*, 2005, **44**, 3112–3120.
49 K. Komatsu, K. Kikuchi, H. Kojima, Y. Urano and T. Nagano, *J. Am. Chem. Soc.*, 2005, **127**, 10197–10204.
50 C. P. Kulatilleke, S. A. de Silva and Y. Eliav, *Polyhedron*, 2006, **25**, 2593–2596.
51 G. K. Walkup, S. C. Burdette, S. J. Lippard and R. Y. Tsien, *J. Am. Chem. Soc.*, 2000, **122**, 5644–5645.
52 C. S. Allen, C.-L. Chuang, M. Cornebise and J. W. Canary, *Inorg. Chim. Acta*, 1995, **239**, 29–37.
53 J. W. Canary, C. S. Allen, J. M. Castanetto and Y. Wang, *J. Am. Chem. Soc.*, 1995, **117**, 8484–8485.
54 J. W. Canary, C. S. Allen, J. M. Castagnetto, Y.-H. Chiu, P. J. Toscano and Y. Wang, *Inorg. Chem.*, 1998, **37**, 6255–6262.
55 J. M. Catagnetto and J. W. Canary, *Chem. Commun.*, 1998, 203–204.
56 L. Zhu, O. dos Santos, C. W. Koo, M. Rybstein, L. Pape and J. W. Canary, *Inorg. Chem.*, 2003, **42**, 7912–7920.
57 J. Zhang, A. E. Holmes, A. Sharma, N. R. Brooks, R. S. Rarig, J. Zubieta and J. W. Canary, *Chirality*, 2003, **13**, 180–189.
58 J. M. Castagnetto, X. Xu, N. Berova and J. W. Canary, *Chirality*, 1997, **9**, 616–622.
59 L. Natrajan, J. Pécaut, M. Mazzanti and C. LeBrun, *Inorg. Chem.*, 2005, **44**, 4756–4765.
60 H. Tsukube, S. Shinoda, J. Uenishi, T. Hiraoka, T. Imakoga and O. Yonemitsu, *J. Org. Chem.*, 1998, **63**, 3884–3894.
61 H. Tsukube, M. Hosokubo, M. Wada, S. Shinoda and H. Tamiaki, *Inorg. Chem.*, 2001, **40**, 740–745.
62 T. Yamada, S. Shinoda, H. Sugimoto, J. Uenishi and H. Tsukube, *Inorg. Chem.*, 2003, **42**, 7932–7937.
63 A. G. Blackman, *Polyhedron*, 2005, **24**, 1–39.
64 I. M. Wasser, C. F. Martens, C. N. Verani, E. Rentschler, H.-W. Huang, P. Moenne-Loccoz, L. N. Zakharov, A. L. Rheingold and K. D. Karlin, *Inorg. Chem.*, 2004, **43**, 651–662.
65 E. E. Chufán, S. C. Puiu and K. D. Karlin, *Acc. Chem. Res.*, 2007, **40**, 563–572.
66 K. Chen and L. Que, Jr, *Angew. Chem., Int. Ed.*, 1999, **38**, 2227–2229.
67 L. Que, Jr and W. B. Tolman, *Angew. Chem., Int. Ed.*, 2002, **41**, 1114–1137.
68 S. L. Tobbey, B. D. Jones and E. V. Anslyn, *J. Am. Chem. Soc.*, 2003, **125**, 4026–4027.
69 S. Zahn and J. W. Canary, *J. Am. Chem. Soc.*, 2002, **124**, 9204–9211.
70 K. Nakanishi and N. Berova, in *Circular Dichroism: Principles and Applications*, eds. K. Nakanishi, N. Berova and R. W. Woody, VCH Publishers, New York, 1994, pp. 361–398.
71 S. V. Psaroudakis and C. E. Efstathiou, *Analyst*, 1989, **114**, 25–28.
72 C. E. Outten and T. V. O'Halloran, *Science*, 2001, **292**, 2488–2492.
73 G. Anderegg, E. Hubmann, N. G. Podder and F. Wenk, *Helv. Chim. Acta*, 1977, **60**, 123–140.
74 N. Wei, N. N. Murthy and K. D. Karlin, *Inorg. Chem.*, 1994, **33**, 6093–6100.
75 M. Royzen, *PhD dissertation*, New York University, New York, 2005.
76 K. Soraka, R. S. Vithanage, D. A. Philips, B. Walker and P. K. Dasgupta, *Anal. Chem.*, 1987, **59**, 629.
77 M. Royzen, A. Durandin, V. G. J. Young, N. E. Geacintov and J. W. Canary, *J. Am. Chem. Soc.*, 2006, **128**, 3854–3855.
78 R. T. Bronson, M. Montalti, L. Prodi, N. Zaccheroni, R. D. Lamb, N. K. Dalley, R. M. Izatt, J. S. Bradshaw and P. B. Savage, *Tetrahedron*, 2004, **60**, 11139.
79 E. M. Nolan and S. J. Lippard, *Inorg. Chem.*, 2004, **43**, 8310–8317.
80 G. K. Walkup and B. Imperiali, *J. Am. Chem. Soc.*, 1997, **119**, 3443–3450.
81 C. J. Fahrni and T. V. O'Halloran, *J. Am. Chem. Soc.*, 1999, **121**, 11448–11458.
82 W. C. Still, P. Hauck and D. Kempf, *Tetrahedron Lett.*, 1987, **28**, 2817–2820.
83 T. Iimori, S. D. Erickson, A. L. Rheingold and W. C. Still, *Tetrahedron Lett.*, 1989, **30**, 6947–6950.
84 S. D. Erickson and W. C. Still, *Tetrahedron Lett.*, 1990, **31**, 4253–4256.
85 P. W. Smith and W. C. Still, *J. Am. Chem. Soc.*, 1988, **110**, 7917–7919.
86 S. Sasaki, H. Naito, K. Maruta, E. Kawahara and M. Maeda, *Tetrahedron Lett.*, 1994, **35**, 3337–3340.
87 H. Tsukube, T. Yamada and S. Shinoda, *Ind. Eng. Chem. Res.*, 2000, **39**, 3412–3418.
88 Z. Dai, X. Xu and J. W. Canary, *Chem. Commun.*, 2002, 1414–1415.
89 H. Irving and R. J. P. Williams, *Nature*, 1948, **162**, 746–747.
90 E. A. Ambundo, M.-V. Deydier, A. J. Grall, N. Aguera-Vega, L. T. Dressel, T. H. Cooper, M. J. Heeg, L. A. Ochrymowycz and D. B. Rorabacher, *Inorg. Chem.*, 1999, **38**, 4233.
91 X. Xu, *PhD dissertation*, New York University, New York, 2000.
92 Z. Dai, *PhD dissertation*, New York University, New York, 2004.
93 Z. Dai, G. Proni, D. Mancheno, S. Karimi, N. Berova and J. W. Canary, *J. Am. Chem. Soc.*, 2004, **126**, 11760–11761.
94 T. Nehira, C. A. Parish, S. Jockusch, N. J. Turro, K. Nakanishi and N. Berova, *J. Am. Chem. Soc.*, 1999, **121**, 8681–8691.
95 A. Ajayaghosh, P. Carol and S. Sreejith, *J. Am. Chem. Soc.*, 2005, **127**, 14962–14963.
96 P. Carol, S. Sreejith and A. Ajayaghosh, *Chem.–Asian J.*, 2007, **2**, 338–348.
97 M. Taki, J. L. Wolford and T. V. O'Halloran, *J. Am. Chem. Soc.*, 2004, **126**, 712–713.
98 Y. Mikata, M. Wakamatsu, A. Kawamura, N. Yamanaka, S. Yano, A. Odani, K. Morihiro and S. Tamotsu, *Inorg. Chem.*, 2005, **45**, 9262–9268.
99 R. P. Haugland, *Handbook of Fluorescent Probes and Research Products*, Molecular Probes Inc., Eugene, OR, 2002.
100 C. J. Chang, E. M. Nolan, J. Jawoski, K.-I. Okamoto, M. Sheng and S. J. Lippard, *Inorg. Chem.*, 2004, **43**, 6774–6779.
101 E. M. Nolan, J. Jaworski, M. E. Racine, M. Sheng and S. J. Lippard, *Inorg. Chem.*, 2006, **45**, 9748–9757.
102 C. R. Goldsmith and S. J. Lippard, *Inorg. Chem.*, 2006, **45**, 555–561.
103 C. C. Woodroofe and S. J. Lippard, *J. Am. Chem. Soc.*, 2003, **125**, 11458–11459.

104 C. J. Chang, J. Jaworski, E. M. Nolan, M. Sheng and S. J. Lippard, *Proc. Natl. Acad. Sci. U. S. A.*, 2004, **101**, 1129–1134.
105 E. M. Nolan, J. W. Ryu, J. Jawoski, R. P. Feazell, M. Sheng and S. J. Lippard, *J. Am. Chem. Soc.*, 2006, **128**, 15517–15528.
106 C. C. Woodroofe, R. Masalha, K. R. Barnes, C. J. Frederickson and S. J. Lippard, *Chem. Biol.*, 2004, **11**, 1659–1666.
107 C. R. Goldsmith and S. J. Lippard, *Inorg. Chem.*, 2006, **45**, 6474–6478.
108 E. M. Nolan, J. Jaworski, K.-I. Okamoto, Y. Hayashi, M. Sheng and S. J. Lippard, *J. Am. Chem. Soc.*, 2005, **127**, 16812–16823.
109 G. Crivat, K. Kikuchi, T. Nagano, T. Priel, M. Hershfinkel, I. Sekler, N. Rosenzweig and Z. Rosenzweig, *Anal. Chem.*, 2006, **78**, 5799–5804.
110 S. Maruyama, K. Kikuchi, T. Hirano, Y. Urano and T. Nagano, *J. Am. Chem. Soc.*, 2002, **124**, 10650–10651.
111 K. Hanaoka, K. Kikuchi, H. Kojima, Y. Urano and T. Nagano, *Angew. Chem., Int. Ed.*, 2003, **42**, 2996–2999.
112 K. Claborn, E. Puklin-Faucher, M. Kurimoto, W. Kaminsky and B. Kahr, *J. Am. Chem. Soc.*, 2003, **125**, 14825–14831.
113 X.-a. Zhang, K. S. Lovejoy, A. Jasanoff and S. J. Lippard, *Proc. Natl. Acad. Sci. U. S. A.*, 2007, **104**, 10780–10785.
114 W.-h. Li, S. E. Fraser and T. J. Meade, *J. Am. Chem. Soc.*, 1999, **121**, 1413–1414.

